

# Towards an Optimal Concept for Numerical Codes Simulating Thrust Chamber Processes in High Pressure Chemical Propulsion Systems

C.-A. Schley, G. Hagemann, G. Krülle

*Deutsche Forschungsanstalt für Luft- und Raumfahrt DLR,  
Lampoldshausen Research Centre, Space Propulsion Division, D-74239 Hardthausen a.K., Germany*

Manuscript received October 12, 1995; revised version February 4, 1996.

---

Schley C.-A., Hagemann G., Krülle G., *Aerospace Science and Technology*, 1997, n° 3, 203-213.

## Abstract

Modelling aspects for rocket engines, where propellants are burned at high pressures to achieve a maximum of performance, are discussed. Concentrating on combustion chamber and expansion nozzle, critical flow phenomena are identified. Physical models for these phenomena with regard to numerical simulations are presented. Different numerical procedures are analyzed concerning their advantages and disadvantages being applied for cryogenic high performance thrust chamber simulations. The application of some of these models is shown exemplarily for a 3D multiinjector combustion chamber and the flowfield computation of a plug nozzle concept to present capabilities, limitations and prospects of CFD in this area. Finally, remarks on verification of numerical schemes with regard to the individual physical, chemical and numerical models are given.

**Keywords:** Computational fluid dynamics – Numerical modelling – Physical modelling – Rocket engines – Rocket thrust chamber flow – Nozzle flow.

---

## LIST OF SYMBOLS

$a$	Constant	$p$	Pressure
$A_t$	Throat area	$Pr$	Prandtl number
$b$	Constant	$\dot{q}$	Specific heat flux
$c$	Mass fraction	$R$	Specific gas constant
$c_p$	Specific heat	$Re$	Reynolds number
$c^*$	$= p_c A_t / \dot{m}$ , characteristic velocity	$T$	Temperature
$C$	Concentration	$U$	Velocity vector
$D$	Diffusion coefficient	$V$	Volume
$h$	Specific enthalpy	$\dot{w}$	Species source term
$I$	Specific impulse	$y^+$	$= y \sqrt{(\rho_w \tau_w) / \mu_w}$ , normalized wall distance
$\dot{m}$	Mass flow	$x, y, z$	Cartesian coordinates
$L$	Length	$\alpha$	Heat transfer coefficient
$M$	Molar mass	$\lambda$	Heat conductivity
$Nu$	Nusselt number	$\mu$	Dynamic viscosity

$\rho$	Density
$\tau$	Shear stress
$\mathfrak{R}$	Gas constant

### Subscripts

$c$	Combustion chamber
$c$	Coolant
$g$	Gas
$h$	Hot
$i$	Index
$0$	Stagnation value
$s$	Specific
$t$	Throat
$w$	Wall

## I – INTRODUCTION AND FOCUS

The reduction of Earth to orbit launch costs in conjunction with an increase in launcher reliability and operational efficiency are the key demands on future space transportation systems. These goals were guiding rules for the Space Shuttle transportation system during the design phase. However, fourteen years of active Space Shuttle service showed that the initial perspectives in cost reduction and reliability were by far too optimistic.

Recent launcher analysis indicate, that the classical, expendable launcher with moderate technological levels, e.g. realized with the ARIANE 5, provide currently the most economical access to space. However, more complex reusable launcher concepts are still subjects of studies, and a great effort has to be spent in this direction to achieve realistic benefits in costs and reliability. Engine concepts for the next generation of transportation systems involve currently used cycles like staged combustion or gas generator, but also advanced cycles, e.g. expander or expander bleed.

To achieve any progress in engine reliability and engine hardware costs, it is of significant advantage to understand basic flow phenomena and combustion processes within the engine. The insight into flow phenomenology helps to understand, and finally to model the essential rate controlling processes. Thus, a reliable numerical simulation of the engine behaviour may lead to a reduction in development time and costs, although hardware tests will never be completely substituted by numerical simulations. As an example *Figure 1* shows a sketch of the Vulcan Mark 1 engine with typical numerical mesh used for a nozzle flow simulation.

Hardware design, its influence on the combustion chamber and nozzle conditions and all relevant physical phenomena must be approximated or represented by models to enable a reliable computational simulation, see *Figure 2*. The degree of model

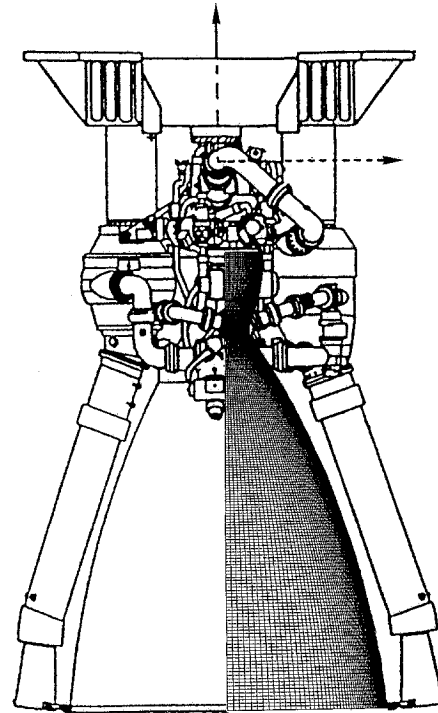


**Fig. 1.** – Sketch of the Vulcan Mark 1 engine with typical numerical mesh used for a nozzle flow simulation.

representativity needed for reliable results strongly depends on the influence of the corresponding problem on chamber processes and is quantitatively not sufficiently known until now in many cases. With regard to the thermophysical conditions in rocket engines, *i.e.* high pressure and density, coaxial injection phenomena, strong temperature gradients, high accelerations as well as strong recirculation zones, many codes use oversimplified assumptions in connection with unsuitable numerical schemes. On the other hand, due to the high chamber pressure which is above the two phase region, some phenomena may be modelled simpler than e.g. in lower pressure combustion engines.

## II – THRUST CHAMBER OPERATION CONDITIONS

Modern high pressure rocket engines such as the European Vulcan engine designed by DASA/SEP shown in *Figure 1* use liquid cryogenic propellants. Typical operation conditions of these engines vary during engine start-up from cryogenic, low pressure two-phase flows, with typical pressures around  $p = 4-10$  bar and temperatures  $T = 20-200$  K, to the stationary operation point, where depending on the engine cycle, maximum pressure are of order of  $p = 160-500$  bar and temperatures ranging up to 3700 K.

A  $H_2/O_2$  rocket chamber injection head consists of a large number of coaxial elements, each of

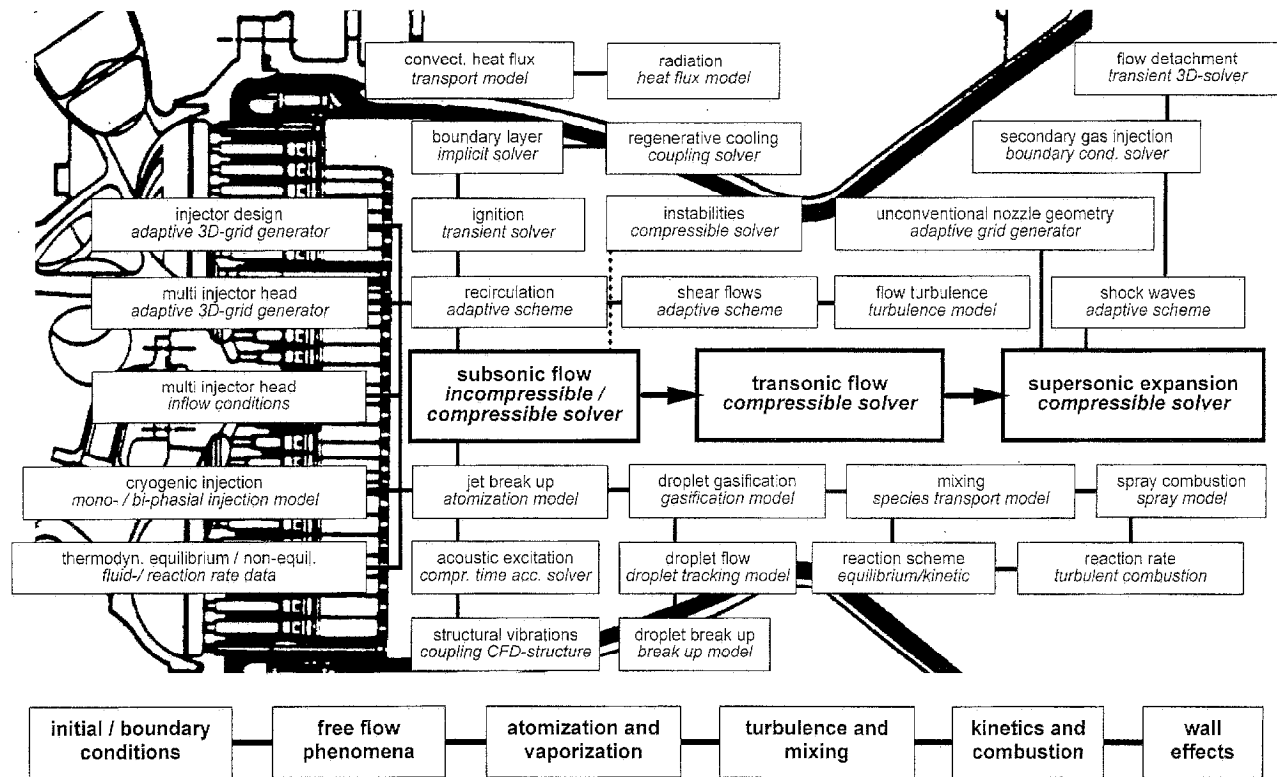


Fig. 2. – Characteristic chamber flow phenomena and derived model requirements for CFD applications in high pressure liquid rocket engines.

which in stationary operation conditions injects a central “liquid”  $O_2$  jet at supercritical combustion chamber pressures around  $p_c = 100\text{-}250$  bar and near critical temperatures of approx.  $T = 100$  K with typical velocities of  $\nu_{O_2,inj} = 20$  m/s surrounded by a fast coaxial gaseous  $H_2$  flow. Typical injection conditions for the hydrogen mass flow are velocities of  $\nu_{H_2,inj} = 200\text{-}300$  m/s and temperatures of  $T = 100$  K for open cycle engines (like gas generator engines, Vulcan type) and  $T = 800$  K for closed cycle engines (like staged combustion engines, SSME type). A typical injection element is shown in *Figure 4*.

The injected dense oxygen core is mixed with the surrounding gas flow and then burned. The involved processes of fluid injection, atomization, mixing and combustion have a decisive influence on rocket engine performance, combustion stability, operational reliability and service life time.

The burned gases are then expanded through the nozzle, while being accelerated from subsonic flow with a typical Mach number of  $M = 0.3$  within the combustion chamber to a Mach number of  $M \geq 4$ , depending on the nozzle exit area ratio.

The essential phenomena are shown in *Figure 2*, together with approaches for the modelling to be discussed in more detail in the following sections.

### III – PHYSICAL MODELLING

*Figure 3* show basic requirements for computational codes with regard to the numerical schemes and the physical modelling for the application on rocket thrust chamber and nozzle flow simulations. Some of these phenomena are adequately simulated by solving the Navier-Stokes equations, whereas others, being not resolved by the numerical mesh, need special models (sub-grid scale models) to be implemented into the numerical scheme. *Figure 5* emphasizes these special models that are discussed in the following.

#### III.1 – Injection

The classical atomization morphology consists of liquid droplets and ligaments being sheared off a liquid jet and then mixed into the environment while evaporating. Recent experiments on cold flow as well as hot firing injection under typical high pressure combustion chamber conditions [10], [15] show, that the distinctive surface and surface tension of the liquid core vanishes when the critical mixing temperature is reached shortly behind the injector. This is a challenge for the algorithms to calculate fluid properties: usually, being restricted to temperatures above 300 K, they have to be extended to the cryogenic range to ensure the correct simulation of the fluid behaviour near the injector, which is of great importance.

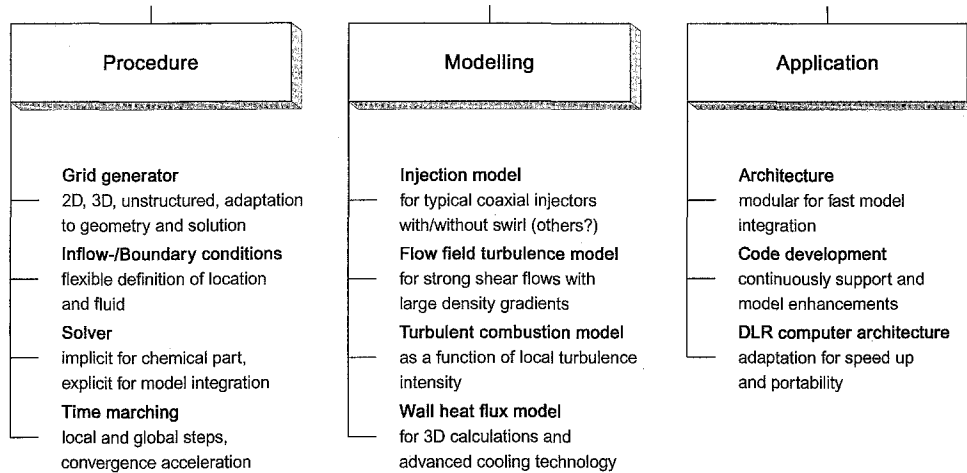


Fig. 3. – Basic requirements to be met by the numerical scheme.

Oxidizer and fuel are mixed within a turbulent dense gas shear layer having large density gradients without any droplets. Therefore, two different categories of injection models can be distinguished in principle for the coaxial injection process:

1. mono-phasic, multi fluid component injection ;
2. bi-phasic, multi fluid component injection.

The first category, the mono-phasic, but multi gas component approximation of the injection process is valid under the assumption that the injection conditions are fully supercritical. This treatment is also applicable if time and length scales needed for heating up the injected liquid to exceed its critical mixing point are very short in comparison to characteristic flow field scales.

The simplest approach to simulate adequately the injection of cryogenic oxygen with a typical density of 1100 kg/m<sup>3</sup> at the injector exit is the *fluid-gas* model, which uses a real gas equation of state like Redlich Kwong [15]

$$p = \rho \frac{\mathcal{R}T}{M(V - b)} - \frac{a}{\sqrt{T} V(V + b)} \quad (1)$$

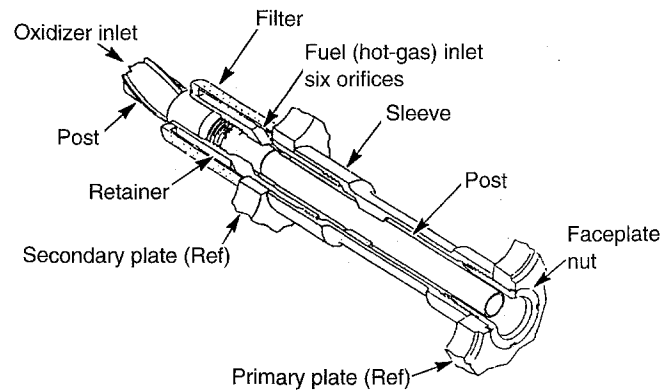


Fig. 4. – Sketch of a typical coaxial injection element (SSME type) [7].

The additional parameters *a* and *b* in comparison to the ideal gas equation of state account for the intermolecular forces and the finite volume of the molecules. The application of this equation to rocket engine injection conditions results in an error in oxygen density of less than 10%, which is quite acceptable, see Figure 6.

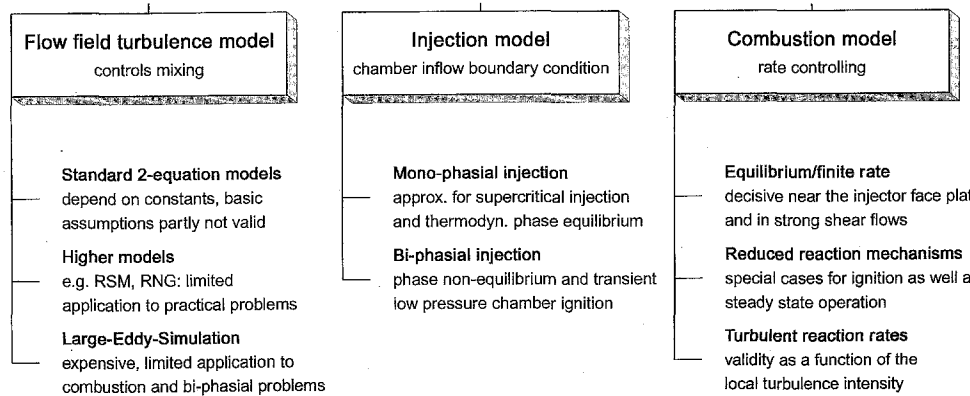


Fig. 5. – Focal points of modelling.

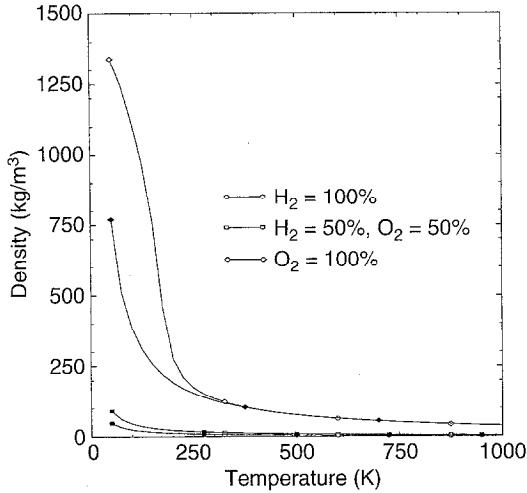


Fig. 6. – Isobars (100 bar) for a H<sub>2</sub>/O<sub>2</sub> mixture with different mixture ratios. Filled symbols: ideal gas equation. Non-filled symbols: real gas equation, Redlich Kwong.

The second category of injection models accounts for two phase flows and droplets which have to be considered during the transient start-up of the engine. Figure 7 shows the corresponding modules that should be implemented into a numerical code. A sub-grid scale model for the primary atomization of the round liquid jet under the influence of strong shear stresses is required. Furthermore, a model for the droplet trajectory and droplet break-up under near and super critical pressure conditions for cryogenic droplets as well as a model for the droplet gasification, ignition and combustion must be implemented. However, it remains questionable if the increased degree of realism gained by the aforementioned two phase flow models results in higher accuracy of the results in comparison with the mono-phasic *fluid-gas* approach, due to limitations in physical modelling of turbulent droplet flows under the described conditions.

Three different liquid core models for bi-phasic injection are summarized in Figure 8. The simplest approach is the *predefined spray* model, which is based on a predefined spray consisting of groups of droplets with a given diameter and velocity distribution, existing already at the injector exit. This model has to

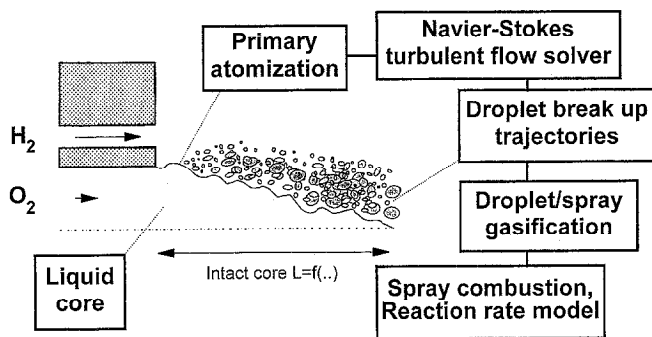


Fig. 7. – Bi-phasic coaxial injection.

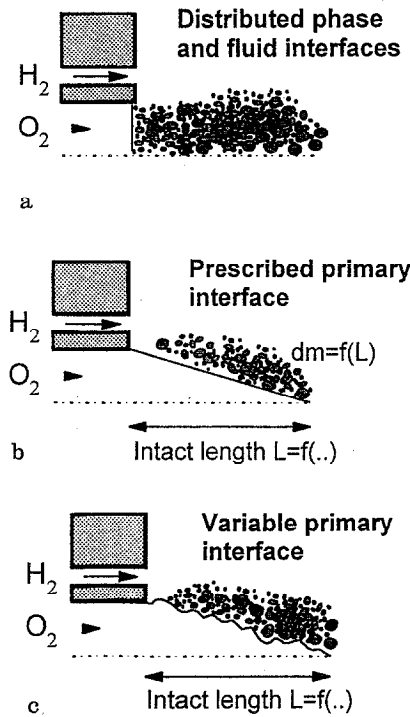


Fig. 8 a-c. – Bi-phasic core models for coaxial injection. a Predefined spray model; b fixed-core spray model; c interactive spray model.

be calibrated for each operation case. A corresponding model is implemented in the KIVA-code [14]. The reliability of this approach remains questionable, since this model does not account for the existing liquid core.

The *fixed core spray* model takes into account the finite time and length needed for the stripping process of the intact liquid core. The modelled shape of the core has to be obtained empirically. Furthermore, the size and velocity distribution of the droplets at the core surface must be calibrated by experiments or derived from reasonable assumptions. The secondary break up must be modelled according to the aerodynamic forces acting on the droplets.

The third bi-phasic model shown in Figure 8, the *interactive spray* model, is the most sophisticated one of these bi-phasic models, which accounts for a variable intact length and droplet distribution. Time dependencies should follow from statistical hypothesis. However, simulations show that this approach may be too time consuming for 3D calculations [11].

### III.2 – Flowfield turbulence

Three different approaches exist in principle for turbulence modelling:

1. statistical methods (zero-, one-, two-equation, higher order schemes),

2. large eddy methods LES,
3. direct numerical simulations DNS.

The latter both require immense computer capabilities and thus are today limited to flow problems with low Reynolds numbers (DNS) or limited physical modelling (LES) [13].

Statistical methods make use of an averaging of the Navier-Stokes equations. However, additional terms appear in the conservation equations, which lead to a closure problem when solving the Navier-Stokes equations. The Reynolds shear stress is in general modelled by the turbulent viscosity approach. Additional terms concerning diffusion and heat conductivity are generally modelled by turbulent Prandtl- and Lewis numbers, respectively. In contrast, the influence of turbulence on species production and dissipation terms and thus on the chemical reaction rates is only crucially approximated with eddy brake-up models. The *flamelet*-approach for turbulent diffusion-flames has to be validated for high pressure combustion chamber processes due to the inherently high level of turbulence. Being rigorous, even a Bunsen burner flame under ambient pressure conditions can not be completely described with the flamelet approach [2]. More sophisticated turbulence models like the *probability density function (pdf)* approach model the turbulent species production terms more accurately, but need a large experimental data base to account for the probability density functions for the special flowfields. Therefore, the latter approach is a subject of on-going research.

For nozzle flow simulations without flow separation and free shear-layer development, algebraic or zero-equation turbulence models give sufficiently accurate results. But with regard to complex flow patterns, transport of turbulent structures cannot be neglected any more. Two-equation turbulence models present here today's state-of-the-art, despite of all their shortcomings.

Two different approaches exist for the numerical simulation of turbulent wall boundary layers and heat flux estimations with a two-equation turbulence model, the wall function approach and the low Reynolds number approach. The wall function approach does not resolve the structure of the boundary layer; the wall nearest point of the numerical mesh is somewhere in the fully developed turbulent boundary layer (generally between  $40 \leq y^+ \leq 100$ ). The flow field variables at these wall nearest points are not calculated with the numerical scheme, but with the wall functions. In contrast, the low Reynolds number approach resolves the turbulent boundary layer down to its laminar sublayer; the flowfield variables within there are calculated directly with the numerical scheme. Thus, the latter approach needs a significantly higher mesh resolution near the walls, since the laminar sublayer (generally below  $y^+ \leq 5$ ) must be resolved.

### III.3 – Ignition and combustion

During the transient start-up of high pressure combustion chambers with ignition of dense liquid spray fields, two-phase flow effects are of dominating influence. The detailed combustion of single droplets can be solved numerically with simplified mathematical models, whereas a modelling of dense spray fields with ignition and droplet combustion is impossible due to limited computer resources even in the near future [16]. Available computer codes which simulate combustion of liquid spray fields assume therefore only a gas-phase combustion [1].

Ignition and combustion under supercritical conditions simplifies the modelling due to the absence of the liquid phase. However, for laminar combustion processes of hydrogen and oxygen, reaction schemes have to be validated for the high pressure regime. A sensitivity analysis of a 26-reaction scheme indicated that at low pressure during the induction period of the combustion, different reactions dominate compared to the intermediate and final stages of the combustion [3]. For high pressures, importance of tri-molecular reactions starts already in the induction period while other reactions dominating at lower pressures are no longer of major influence [3]. Despite these uncertainties in the reaction schemes, another dominating parameter, the turbulence, has to be taken into account for ignition and combustion modelling, as already discussed in the preceding chapter.

For numerical simulation of steady state conditions in the combustion chamber, the mixing of oxidizer and fuel acts as rate controlling parameters [8], [14]. Thus, combustion modelling based on a "mixed-is-burned"-hypothesis with equilibrium chemistry and a temperature threshold seems to be an adequate simplification.

### III.4 – Sub- and supersonic expansion

During the expansion process through the combustion chamber and nozzle extension, burned gases are accelerated from subsonic flow velocities to trans- and supersonic velocities, see *Figure 2*. Main losses in the nozzle originate from chemical non-equilibrium effects, friction, divergence and shocks [9]. Furthermore, flow separation may occur. Imperfections in mixing, vaporization and combustion in the combustion chamber leading to a stratified mixture ratio distribution during the expansion as well as multi-phase flows through the nozzle induce additional losses. Friction losses and divergence losses are implicitly considered when solving the Navier-Stokes equations in a 2D- or 3D-form. Additionally, flow separation can also be accurately predicted, depending on the turbulence model.

In case of chemically reacting gases, special models have to be considered to evaluate the equation of state for ideal gases. Different approaches exist:

1. frozen flow with constant or temperature dependent specific heat,
2. local chemical equilibrium,
3. following the *Bray*-criterion, local chemical equilibrium down to the throat area, and frozen flow further downstream,
4. chemical non-equilibrium with finite reaction rates (highly CPU-time-consuming, depending on the number of species).

Chemical non-equilibrium effects have an important influence on rocket nozzle performance for low pressure rocket engines, whereas their influence can be neglected in high pressure rocket nozzles with chamber pressures above 100 bar [9]. The expansion within these nozzles can be reasonably simulated with the assumption of a local chemical equilibrium composition throughout the nozzle [5]. However, it must be remarked that heat fluxes are drastically overestimated when using the chemical equilibrium assumption, which will be discussed in the following section.

### III.5 – Wall heat flux

The accurate prediction of the wall heat flux is not solved yet, but is of great importance for high pressure liquid rocket engines, since an underprediction of wall temperatures can significantly decrease chamber and nozzle lifetime. Thus, modelling should be performed with detailed models for the hot gas side heat flux to the wall, and the heat flux through the wall to the cooling gas in a coupled, iterative procedure. However, most uncertainties exist on the hot gas side heat flux, which is regarded in more detail in the following.

Two fundamental different approaches exist for wall heat flux calculations of the hot gas side. The first one, known as engineering approach, deduces the heat flux estimation to a 1-D problem, *Figure 9*

$$\dot{q} = -\alpha(T_{0g} - T_{wh}) \quad (2)$$

where the heat transfer coefficients result from empirical correlations, depending on the Reynolds- and Prandtl number. The necessary flow data follow from one- or multi-dimensional Euler calculation with slip condition at the wall. Uncertainties in

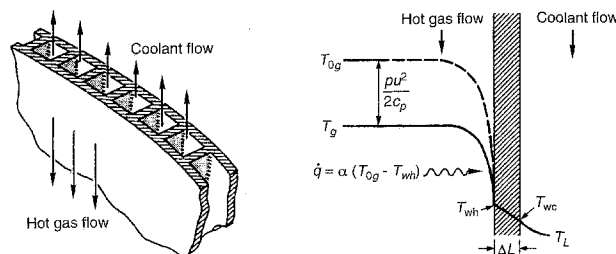


Fig. 9. – Sketch of combustion chamber and nozzle flow with one-dimensional heat flux model [6].

this approach arise from the validity of the used correlations, especially with regard to the three dimensional combustion chamber flow with local hot spots near the wall and possible boundary layer collapse.

The second approach follows from an energy balance of the hot gas side at the wall:

$$\dot{q} = -\lambda \nabla T + \sum_i \rho_i U_i h_i. \quad (3)$$

The term with the species diffusion is in general modelled using Fick's law for multispecies reacting gas flows consisting of *ns* species:

$$\rho_i U_i = -CD_i \nabla \left( \frac{\rho_i}{C} \right) + \left( \frac{\rho_i}{\rho} \right) \sum_{k=1}^{ns} CD_k \nabla \left( \frac{\rho_k}{C} \right). \quad (4)$$

Finally, this leads to

$$\dot{q} = -\lambda \nabla T - \sum_i \left( CD_i h_i \nabla \left( \frac{\rho_i}{C} \right) + \left( \frac{\rho_i}{\rho} \right) h_i \sum_{k=1}^{ns} CD_k \nabla \left( \frac{\rho_k}{C} \right) \right) \quad (5)$$

or, simplified with equal diffusion coefficients for all species,  $D_i = D_k = D$

$$\dot{q} = -\lambda \nabla T - \sum_i \left( \rho D h_i \nabla \left( \frac{\rho_i}{\rho} \right) \right). \quad (6)$$

Laminar transport properties for heat conductivity  $\lambda$  and species diffusion  $D_i$ , together with temperature- and mass fraction gradients, the latter both strongly influenced by turbulence (*see* turbulence modelling), are needed for accurate heat flux predictions. The following approaches for modelling exist:

- a two- or three-dimensional analysis of the viscous and inviscid flow regimes together with a detailed resolution of the boundary layer down to its laminar sublayer.

Problem: → immense CPU-time requirements due to a strong grid refinement in wall-normal and both-tangential directions near the wall

- separation of viscous inviscid flow regime with an individual, mathematically optimized treatment of both flow regimes.

Problem: → the correct prediction of the coupled influence of both flow regimes on each other.

The remaining uncertainty is the choice of a proper boundary condition for the catalytic behaviour of the wall with regard to the reaction rates, and thus to the gradient of the species mass fractions:

- full catalytic wall  $c_i = c_{i \text{ equilibrium}}$ ,
- non catalytic wall  $\frac{\partial c_i}{\partial y} = 0$ ,
- partially catalytic wall  $(\dot{w}_c)_i + \rho_i U_i = 0$ .

Upper and lower limiting values for the heat flux can be calculated with the fully catalytic and non-catalytic wall behaviour. The more realistic partially catalytic assumption has its inherent disadvantage in the species production term  $(\dot{w}_c)_i$ , which in general can not be modelled adequately at the moment.

#### IV – NUMERICAL MODELLING

Different numerical simulation schemes including commercial ones have been checked for their applicability to compute in-chamber processes of high pressure chemical propulsion systems [14]. Despite good theoretical performance, most of the tested schemes are not suitable for that purpose due to limitations in physical or numerical modelling.

On the other hand, some simulation schemes applied to compute e.g. the temperature and species distribution in 3D show, that the dependency of the in-chamber conditions on boundary conditions or variation of the chamber- as well as injector-design is computed qualitatively correct.

##### IV.1 – Grid generation

The grid should be locally adaptive, unstructured or at least block-structured to resolve all details of the injector face plate consisting of several injector elements in the 3D case. The ratio of a typical chamber length to the LOX-post tip thickness is of three to four orders of magnitude. This has to be resolved sufficiently to reproduce the experimentally well observed influence of the injector design on the chamber flow pattern adequately. It is only possible in 3D with an unstructured or structured but locally adaptive scheme with respect to acceptable CPU-times. The same difficulty arises with respect to strong flow field gradients and the resolution of weak but important recirculation areas near the walls and the injector face plate. Required CPU-times would be prohibitive for purely structured schemes resolving all hardware and flow field phenomena in 3D with a mesh independent solution (mesh convergence!).

##### IV.2 – Solution algorithm and code formulation

The type of the solver has an important influence on criteria like convergence, model integration and boundary layer treatment. Incompressible or weakly compressible solver where the density depends only on temperature and not on pressure converge comparably faster than compressible schemes in the large subsonic part of the combustion chamber, but have stability problems when computing the fully compressible supersonic expansion. The implicit treatment of the equations allows to resolve the boundary layer down to the laminar sublayer and hence the direct computation of the local wall heat flux without the application of empirical  $Re/Nu/Pr$  formulas. Explicit codes are much

better suited for fast model integration and testing, but slow down drastically with decreasing mesh size due to the CFL-stability criterion.

##### IV.3 – Boundary conditions

Flexibility in the definition of the injection location and choice of the injected cryogenic fluid, fluid properties as well as the correct formulation of the subsonic inflow boundary condition for both fluids is crucial for the correct representation of the chamber inflow. This is of major importance for the complete combustion chamber flow pattern. Simple supersonic inflow conditions not reacting on the combustion chamber condition, e.g. pressure variations, lead to non-realistic results. To compare with experiments, the inflow conditions (e.g. turbulence conditions at the injector exit) should be known as exactly as possible.

#### V – SIMULATION EXAMPLES

##### V.1 – Rocket combustion chamber

The presented chamber simulation has been performed using an explicit finite-volume code that solves the three-dimensional, time-dependent Navier-Stokes equations. The development of this code was specially focussed on the injection and combustion modelling [4, 14, 15]. The numerical scheme has a local grid refinement capability, which is of advantage for its application to the rocket combustion chamber. *Figure 10* shows two temperature distributions inside a model combustor where the only source of difference is the tip design of the LOX-post. Due to different flow fields at the end of the injectors, the mixing zones in the wake of the injectors are much shorter, and the homogeneity of the combustion within the chamber is fairly enhanced. The code is capable of resolving the different evolution of shear layers behind each coaxial injector due to flow field adaptation and hence to simulate the response of the in-chamber condition on different turbulence levels generated at the injector outlet. The increased turbulence level leads to a much shorter length required for the mixing of both propellants and results in a more homogeneous temperature distribution within the chamber.

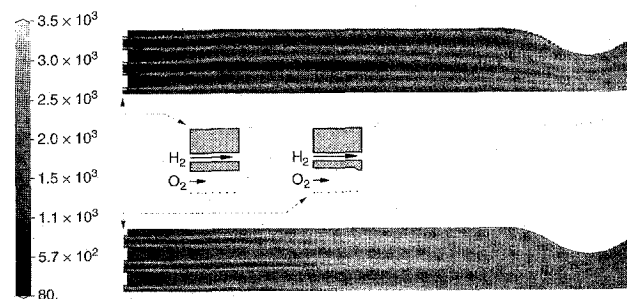


**Fig. 10.** – 3D in-chamber temperature of a 19-injector engine depending on LOX-post design.

Additionally, the wake flow of a coaxial injector and thus the flame holding process – the flame is directly attached to the LOX-post – is predicted in all simulated cases in good agreement to experiments performed with chamber pressures between 15 bar and 100 bar [10]. Other codes that have been checked reveal in some cases a totally different flame behaviour, e.g. a flame tip lifted of the injector which is in disagreement to the experiments [10].

## V.2 – Rocket nozzle

An experimentally tested plug nozzle is chosen as an example for the numerical simulation of rocket nozzles. All phenomena with regard to propellant injection, atomization and combustion are neglected in this numerical simulation. A homogeneous inflow is assumed through the combustion chamber. The three-dimensional Navier-Stokes equations are solved for an ideal gas with constant specific heats; turbulence is simulated with a high Reynolds number two-equation model, see [12] for further details.

Figure 11a shows a photograph of an experiment performed at DLR Lampoldshausen with a toroidal plug nozzle, using a propellant combination of gas-oil and nitric acid. The thrust level of the toroidal rocket chamber with the plug nozzle was 15 kN. The photo of the experiment gives a total of the flowfield, whereas Figure 11b shows the calculated Mach number distribution in the cross section of the centerline. The predicted flowfield is in good overall agreement with the experiment. Flow separation from the plug contour and the formation of three Mach discs can be observed. However, the exact prediction of the separation point has to be investigated further with other turbulence approaches.

a) (below) toroidal plug nozzle experiment with gas-oil/nitric acid propellant combination, side view photograph  
b) (right) computational results of toroidal plug nozzle, Mach number distribution, full gray and isolines, centreline section

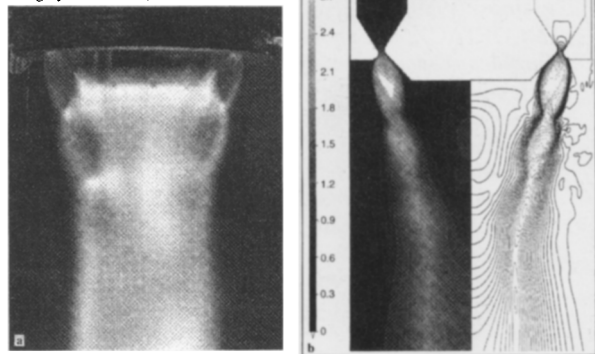


Fig. 11. – Plug nozzle flowfield: experiment vs numerical simulation (description at the top left).

## VI – VERIFICATION

A code consisting of a multitude of physical and numerical models influencing each other has to be fundamentally verified to create and ensure confidence with respect to the results. Application of a computational scheme as predictive design tool is only justified if the results compare qualitatively and quantitatively well with observed trends and experimental evidence. Each decisive submodel has to be compared with basic experiments. Verification has not to rely only on expensive hot runs. The injection model, single phase multi fluid as well as two phase flow models, can be verified using a high pressure injection test stand with cryogenic nitrogen simulating the oxidizer flow and matching all relevant similarity parameters [15]. The neglect of the flame zone results in no significant change to parameters of rate controlling importance for the primary atomization. The same can be done as a first approximation for the turbulent mixing model, that has to be validated for strong shear flows and large density differences between oxidizer and fuel. In the latter case, verification has also to be done in the hot case to check if the volume expansion of the turbulent mixing layer due to the flame zone is properly modelled. Additionally, the combustion model for turbulent diffusion and premixed flames taking into account very low temperatures near the injector can be verified only under firing conditions.

Different degrees of verification can be distinguished for most of the models:

1. Global verification: no optical insight into the model combustion chamber is required. Measurement of the chamber pressure gives a global information about the overall efficiency, expressible by the characteristic velocity  $c^*$ , which can be compared to simulation results. Additionally, measurement of local wall heat fluxes gives insight into macroscopic length scales required for mixing and burning.

2. Qualitative verification: optical access into the combustion chamber is required for phenomenological studies. The appearance of the dense core regime in cold flow tests and the flame shape during hot runs can be analyzed.

3. Quantitative verification: optical access for the application of advanced laser diagnostics is required. For the cold case, a pdf e.g. of the oxidizer mass fraction can be generated for different locations within the measuring chamber and compared to computational results. During hot firing tests, species distribution of rate controlling radicals as well as temperature pdf's will give quantitative information about the mixing and combustion process, see Figure 12.

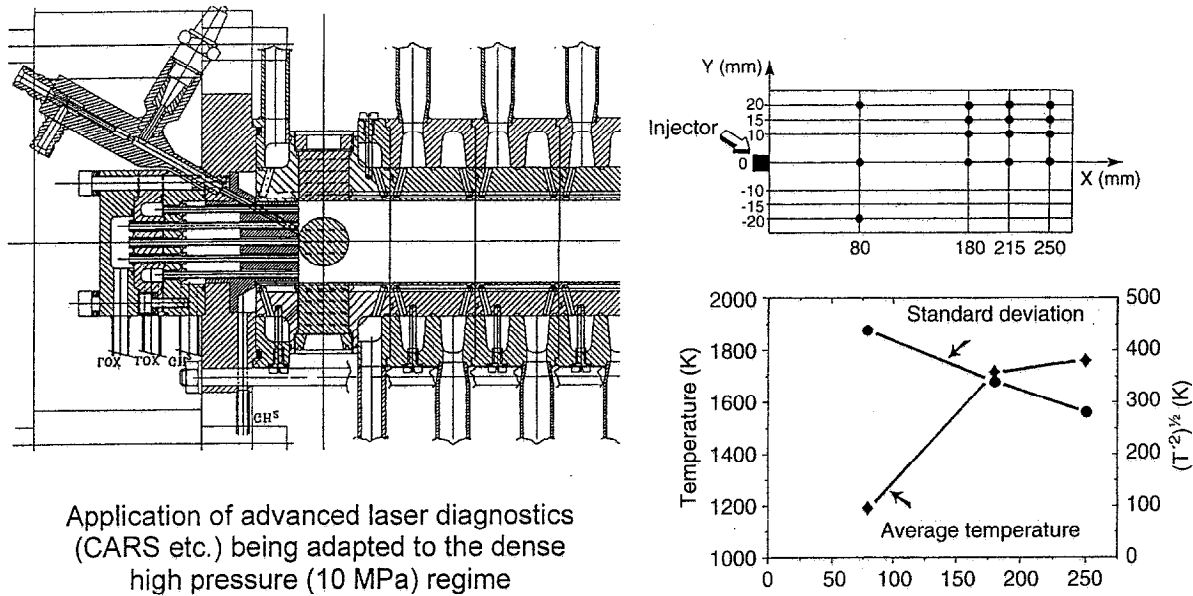


Fig. 12. – Quantitative verification: sub-scale combustion chamber (top) and measurements (bottom).

## VII – CONCLUSIONS AND FURTHER WORK

Numerical schemes simulating thrust chamber processes of high performance chemical propulsion systems have been reviewed. Results show that their applicability as a predictive tool for quantitative combustion chamber design purposes is limited due to shortcomings in physical modelling and numerical treatment. Modelling of decisive rate controlling phenomena occurring inside the combustion chamber, see *Figure 2*, has not reached a satisfactory status until now to ensure quantitatively reliable results. For nozzle flows, in contrast, results obtained with state of the art tools compare even quantitatively well with experimentally obtained results.

The only optimal concept, *i.e.* one global code simulating all physical processes from injection to wall heat flux, will not exist for a considerable time. Different aims and applications require the specialization of the numerical scheme on different subjects. E.g. to determine the wall heat flux inside the subsonic combustor efficiently, a weakly compressible and implicit scheme is preferable. This scheme would fail when being applied to compute the flow field and also the heat flux in the transsonic part near the nozzle throat, where a fully compressible scheme is required. For model integration and testing purposes, an explicit code has advantages despite being incapable of boundary layer calculations in 3D.

On the other hand, present capabilities show that it is possible to simulate in 3D combustion chamber effects, that can also be observed in the full scale hot run experiment.

The stratified mixture zone in the wake of the coaxial injector is predicted qualitatively correct. The flame holding process directly behind the LOX-post

of each injector matches exactly with experimental observations. The response of the combustion chamber flow pattern on different injector designs or different arrangements and distributions of injectors at the injector face plate shows qualitatively correct results, e.g. hot spots at certain locations on the wall which tend to overstress the wall structure.

Therefore, suitable computational schemes may be applied even today within the design process for a first optimization. Nevertheless, experimental fine tuning is furthermore required until physical models describe decisive phenomena – injection, atomization, mixing, combustion – in a more accurate quantitative way.

## REFERENCES

- [1] Amsden A. A., O'Rourke P. J., Butler T. D. – *KIVA II: A Computer Program for Chemically Reactive Flows with Sprays*. Los Alamos National Laboratory, Los Alamos, 1989.
- [2] ERCOFTAC. – *Summer School on Laminar and Turbulent Combustion*, Aachen, Germany, 1992.
- [3] Golovitchev V., Schley C.-A., Krülle G. – Ignition Sequence and High Pressure Steady State Simulation of  $H_2/O_2$  Combustion at Model Engine Thrust Chamber Conditions. *Conference on Propulsive Flows in Space Transportation Systems*, Bordeaux, France, 1995.
- [4] Gavrilyuk V., Denisov O., Nakonechny V., Odintsov E., Sergienko A., Sobachkin A. – Numerical Simulation of Working Processes in Rocket Engine Combustion Chamber, *IAF-93-S.2.463*, Graz, Austria, 1993.
- [5] Hagemann G., Krülle G., Hannemann K. – Numerical Flowfield Analysis of the Next Generation Vulcan Nozzle, *AIAA-95-2782*, San Diego, California, 1995.

- [6] Hill Ph., Peterson C. – *Mechanics and Thermodynamics of Propulsion*, Addison-Wesley Publishing Company, 1992.
- [7] Huzel D. K., Huang D. H. – Modern Engineering for Design of Liquid-Propellant Rocket Engines, *Progress in Astronautics and Aeronautics*, AIAA, 192.
- [8] Liang P. Y., Fisher S., Chang Y. M. – Comprehensive Modelling of a Liquid Rocket Combustion Chamber, *J. Propulsion and Power*, 2, 1986.
- [9] Manski D., Hagemann G. – Influence of Rocket Design Parameters on Engine Nozzle Efficiencies, *AIAA-94-2756*, Indianapolis, Indiana, 1994.
- [10] Mayer W., Tamura H. – Flow Visualization of Supercritical Propellant Injection in a Firing LOX/GH<sub>2</sub> Rocket Engine, *AIAA-95-2433*, San Diego, California, 1995.
- [11] Mayer W. – Zur koaxialen Flüssigkeitszerstäubung im Hinblick auf die Treibstoffaufbereitung in Flüssig-Raketentriebwerken, *DLR-FB 93-09*, 1993.
- [12] Rommel Th., Hagemann G., Schley C.-A., Manski D., Krülle G. – Plug Nozzle Flowfield Calculations for SSTO Applications, *AIAA-94-2784*, San Diego, California, 1995.
- [13] Schley C.-A. – Large-Eddy-Simulation of Turbulence in High-Pressure H<sub>2</sub>/O<sub>2</sub> Rocket Engine Injectors and its Effects on LOX-Jet Atomization, *AIAA-94-2776*, Indianapolis, Indiana, 1994.
- [14] Schley C.-A., Hagemann G., Golovitchev V. – Comparison of High Pressure H<sub>2</sub>/O<sub>2</sub> Rocket Model Engine Reference Simulations, *AIAA-95-2429*, San Diego, California, 1995.
- [15] Schley C. A., Shik A., Krülle G. – Cryogenic High Pressure Coaxial Injection and Atomization: Experiments and Modelling, *AIAA-95-2556*, San Diego, California, 1995.
- [16] Warnatz J., Maas U. – *Technische Verbrennung*, Springer-Verlag, 1993.